Nucleation and Growth of Monodisperse Droplets in a Binary-Fluid System

Andrew Cumming and Pierre Wiltzius
AT&T Bell Laboratories, Murray Hill, New Jersey 07974

Frank S. Bates
Department of Chemical Engineering and Materials Science, University of Minnesota, Minneapolis, Minnesota 55455
(Received 8 March 1990)

Mixtures of polyisoprene and poly(ethylene-propylene) have been studied using time-resolved elastic light scattering. For off-critical quenches just into the two-phase coexistence region, highly monodisperse spheres are observed, whose radii grow with a power law $R(t)=R_0 t^{1/2}$. The monodispersity and growth law are explained as a heterogeneous nucleation process with a simple model equation for the growth of isolated spheres, and allow the study of the kinetics of domain growth for metastable thermodynamic processes in unprecedented detail.

PACS numbers: 61.25.Hq, 05.70.Fh, 64.60.Qb, 64.75.+g

The behavior of binary systems which may phase separate has been a paradigm for both the theoretical and experimental study of phase transitions and critical phenomena for many years. Polymer blends have recently emerged as a particularly useful subclass of such systems insofar as the dynamics of phase separation can be investigated on time scales easily accessible in the laboratory. Low-molecular-weight systems, such a lutidine water and isobutyric acid water, rely on critical slowing down to render their time-dependent behavior measurable in a quench experiment.[1,2] In this Letter, we report the observation of a novel phase-separation phenomenon in a blend of polyisoprene (PI) and poly(ethylene-propylene) (PEP) with molecular weights of 2000 and 5000, respectively. This system has an upper critical solution temperature phase diagram with a critical temperature $T_c=38\,^\circ$C, and critical composition $\phi_c=0.605$ volume fraction PI. This intermediate-molecular-weight system allows temperature quenches $0.05\lesssim\Delta T\lesssim 5\,^\circ$C below the binodal into the metastable or unstable regions of the phase diagram, bridging results obtained with simple fluid systems[1,2] ($\Delta T\lesssim 0.01\,^\circ$C) and recent work with high-molecular-weight polymers[3,4] ($\Delta T\gtrsim 2\,^\circ$C).

For sufficiently shallow off-critical quenches, ΔT in the range 0.15–1.06 °C, we observe the nucleation of spherical droplets of the minority phase. We have determined that for times of order 10^2–10^4 s, the spheres are highly monodisperse (polydispersity $\lesssim 3\%$), and the radius grows as $R(t)\sim t^{1/2}$. The observation of this growth law is entirely new for phase-separating quenched binary systems. For significantly longer times, the polydispersity increases, while for deeper quenches, the separating phases enjoy a distinctly different morphology, akin to the bicontinuous percolated phases encountered in spinodal decomposition.

Elastically scattered laser light $I(q)$ was measured with a 14-bit 512×512 charge-coupled device. The typical measuring time for $I(q)$ over momentum transfer $2000\lesssim q\lesssim 75000$ cm^{-1} is 1 s or less. Azimuthal averaging in q space resulted in an effective dynamic range of five decades in intensity. The temperature-control system, which will be described elsewhere, provided 20-mK stability at both the prequench and postquench temperatures, with quench times on the order of 30 s.

The large viscosity of the polymer mixtures prevents macroscopic phase separation on laboratory time scales. It is thus not practical to measure the coexistence curve directly by allowing complete separation. Instead we estimated the coexistence curve shown in Fig. 1 by slowly

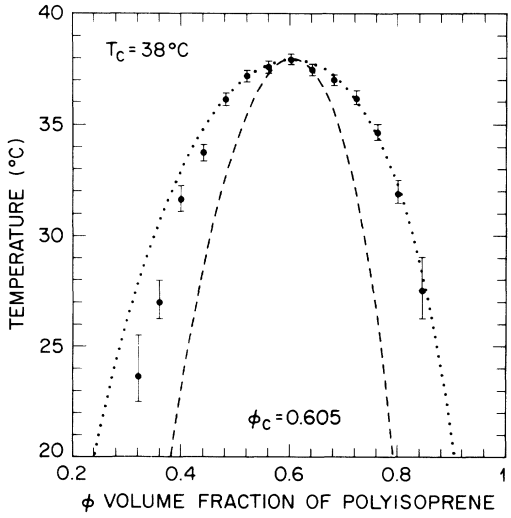

FIG. 1. Phase diagram for polyisoprene-poly(ethylene-propylene) system used to study phase-separation dynamics of off-critical quenches. The results communicated in this paper are for the sample at $\phi_{PI}=0.48$. The dashed and dotted curves are the spinodal and binodal curves, respectively, for a best-fit Flory-Huggins free-energy-density calculation. The data are the experimentally measured phase-separation thresholds for a variety of different concentrations.

cooling the samples until they were observed to scatter strongly in the forward direction. The dashed and dotted curves represent the spinodal and coexistence curves, respectively, for a best-fit free-energy density of the Flory-Huggins form:[5]

$$f(\phi)=\frac{\phi\ln\phi}{N_{\mathrm{PI}}}+\frac{(1-\phi)\ln(1-\phi)}{N_{\mathrm{PEP}}}+\chi\phi(1-\phi). \quad (1)$$

$N_{\mathrm{PI}}=29$ and $N_{\mathrm{PEP}}=73$ are the known polymerization indices of the two species and $\chi=a/T+b$ is the Flory interaction parameter,[5] wherein $a=51.9$ and $b=-0.12$ are fitting parameters, determining T_c and the width of the coexistence curve. Note that $\phi_c=\sqrt{N_{\mathrm{PEP}}}/(\sqrt{N_{\mathrm{PI}}}+\sqrt{N_{\mathrm{PEP}}})$ is not a fitting parameter.[6] Inside the spinodal, infinitesimal concentration fluctuations will grow exponentially,[7] and the system is said to be unstable. In the region between the spinodal and the coexistence curves the system is metastable because although small-amplitude concentration fluctuations decay, large enough ones will grow. The phase-separation processes in these regions are termed *spinodal decomposition* and *nucleation and growth*, respectively.

Here we are primarily concerned with the phase-separation dynamics for quenches to various depths at the off-critical concentration $\phi=0.48$. Figure 2 is a semilogarithmic plot of $I(q)$ 8000 s after a quench 0.64 °C below the coexistence curve at this composition. The data, represented by the open circles, are characteristic for sufficiently shallow quenches into the coexistence region with $0.15\leq\Delta T\leq 1.06$ °C. They have been multiplied by a factor of 2 to displace them from the model curves for clarity. The dash-dotted curve is a two-parameter fit to the data of a model calculation in the first Born approximation of the form factor for dielectric spheres[8] with Gaussian-distributed radii, and no coherent effects between spheres. The half-width of the distribution is 3% of the peak position. The two fitting parameters are the mean of the radius distribution (3.16 μm for the case shown) and the intensity prefactor of the function (in arbitrary units). The other curves are plots of the model function for half-widths 0%, 7%, and 12% of the same mean radius, and with the same intensity. The model curves show that if the fourth- and fifth-order resonances are not to be washed out by polydispersity, the half-width of the radius distribution is limited to around 3% of the mean. We attribute the failure of the 3% curve to correctly account for the low-q node depths to multiple scattering from the relatively bright low-order resonances or to forward scattering from unavoidable dust particles.

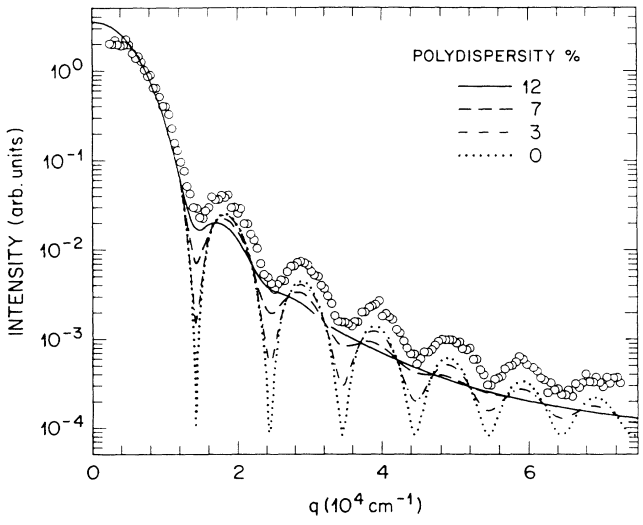

FIG. 2. $I(q)$ for scattering from a nearly monodisperse distribution of spheres. The open circles are data and the curves are a model calculation from spheres with Gaussian-distributed radii, with polydispersity ($=\sigma/\mu$) 0%, 3%, 7%, and 12%. To model successfully the high-order resonances, one is limited to polydispersity on the order of 3%.

The scattered intensity can be written as $I(q)=P(q)S(q)$, where $P(q)$ is the form factor of the individual scatterer and $S(q)$ is the structure factor of the scatterers. Deviations in the near-forward direction in Fig. 2 are consistent with either a suppressed $S(q)$ due to coherent effects between spheres, or the modification of $P(q)$ due to the existence of a concentration depletion zone around the spheres. Using an optical microscope, we were able to determine the spacing between droplets, which varies in the range 20–200 μm. One gets the distinct impression of random placement of these spherical domains of minority phase, suggesting an $S(q)$ near unit for all measurable q. We thus tend to attribute the deviations between $I(q)$ and the calculations to the depletion zone.

Figure 3 is a logarithmic plot of the time dependence

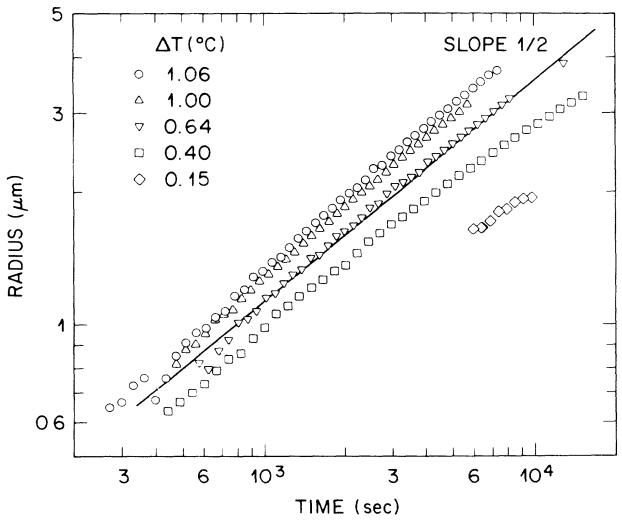

FIG. 3. Logarithmic plot of the mean sphere radius as a function of time for several quench depths in the range 0.15–1.06 °C. A line of slope $\frac{1}{2}$ is shown for comparison.

of the radius of the spheres for several quenches at $\phi=0.48$. A line with slope $\frac{1}{2}$ is plotted for comparison. Though it is evident that a $t^{1/2}$ law is approximately obeyed throughout, there may be a gradual crossover from a slightly larger to a slightly smaller exponent. For quenches slightly deeper than the deepest shown in Fig. 3 (1.06 °C), there is an abrupt change in behavior. In the very earliest times the spherical form factor can be measured, but it is quickly overwhelmed by the characteristic ring which brightens and shrinks in radius with time according to the $t^{1/3}$ law expected for Lifshitz-Slyozov (LS) coarsening[9] and spinodal decomposition.[10] Under the optical microscope, we also initially observe the formation of droplets. After a short time, however, the supersaturated sea surrounding the droplets develops an instability in the concentration field and a morphology reminiscent of that of spinodal decomposition develops. This happens when we observe a spinodal ring form in the scattered light signal. This quench depth is a factor of 3 shallower than the position of the classical spinodal as calculated in the best-fit Flory-Huggins free-energy density for this concentration (see Fig. 1). It is notable that the sample does not become cloudy to the naked eye for quenches shallower than this, even when allowed to sit for several days. We conclude that this is the cloud point, and that to observe nucleation and growth unfettered by more complicated phenomena, one must limit the quench depth to avoid this region. Other investigators, by contrast, have only observed the dynamics below the cloud point because they have required the higher scattering signals encountered there to make measurements.[11] These observations confirm the recent emphasis by Hayward, Heermann, and Binder[12] that spinodal decomposition behavior is to be observed at significantly smaller initial supersaturation than represented by the classical spinodal.

A rate equation for the radius of an isolated droplet in a sea of supersaturated phase can be derived by solving the diffusion equation with the appropriate spherical boundary conditions:[9,13]

$$\frac{dR}{dT}=\frac{D}{R}\left(\Delta-\frac{\alpha}{R}\right), \tag{2}$$

where R is the sphere radius, D is the diffusion coefficient, Δ is the relative supersaturation, and α is the capillary length. Clearly if $R<R^*=\alpha/\Delta$, then the radial rate of growth is negative, and the droplet evaporates, whereas for $R>R^*$, the droplet is viable and will grow.

Equation (2) can be rewritten in terms of reduced variables ρ and τ defined as follows:

$$\rho=\frac{R}{R^*}=\frac{\Delta}{\alpha}R, \quad \tau=\frac{D}{\alpha^2}\Delta^3 t. \tag{3}$$

Provided the system-dependent parameters, such as D and α, do not vary appreciably over the range of temperatures sampled, a simple rescaling of the axes in Fig. 3 should bring all the quench data onto a single curve. Figure 4 is a replot of the data in Fig. 3 with the time axis rescaled by $\alpha^2/D\Delta^3$ and the radius axis rescaled by R^*. The supersaturation Δ was calculated using the quench temperatures. For this system, $D=9\times10^{-11}$ cm^2/s, as measured by dynamic light scattering outside the coexistence curve.[14] R^*, hence α, were calculated using a theory of Binder,[15] and estimates for the interfacial tension were according to Joanny and Leibler.[16] α is approximately 20 Å, which is $\frac{1}{3}$ of the correlation length, as expected.[15,17] The solid curves represent integrations of the dimensionless version of (2) for initial data scattered on the interval $\rho\in(1,5]$ at $\tau=10$. Δ is held constant for these trajectories, consistent with the hypothesis that the droplets are noninteracting. There are no adjustable parameters in this fit. The remarkable feature is that an initially polydispersive droplet distribution has developed into a sharp distribution when the earliest measured reduced time is reached. The lack of data points for $\tau\leq80$ in Fig. 4 is not accidental. We did indeed measure $I(q)$ for the $\Delta T=0.15$ °C quench at times $t<6000$ s. The minima for these $I(q)$ are, however, washed out to a point where the average sphere radius cannot be determined, consistent with a polydispersity greater than 12%. The late-time deviation may be attributable to the slowing of the growth as the supersaturation decreases.

The intensity of forward-scattered radiation from a dielectric sphere scales as the square of its volume.[8] For the total scattering from a collection of such spheres, we have then $I(q=0)\sim nR^6$, where n is the number density of the spheres. Our intensity data are well fitted with the

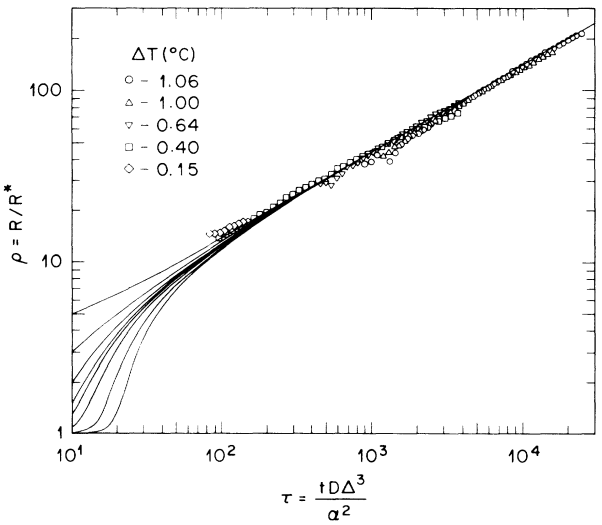

FIG. 4. Plot of data in Fig. 3 with the time axis rescaled by $\alpha^2/D\Delta^3$ and the radius axis rescaled by R^*. The model curves are numerically integrated solutions of (2) for various initial conditions, showing that the monodispersity is a natural consequence of free growth of nucleated droplets once the nucleation has stopped.

sixth power of the radius, indicating that the number density remains constant for $\tau \gtrsim 100$. This situation deviates from that described in the homogeneous nucleation theory of Langer and Schwartz[17] in that the nucleation rate drops to near zero after some early time, independently of the quench depth. These observations are consistent with a heterogeneous nucleation picture in which there is a fixed number of sites that are preferentially wetted by the minority phase. We expect that at late time (months with these fluids) there would be crossover to LS coarsening with its attendant onset of a polydisperse droplet radius distribution and the $t^{1/3}$ growth law. For the 0.15 °C and 0.40 °C quenches, the long-time limit of the data sets shown in Fig. 3 were determined when the polydispersity became sufficiently high that an average radius could not be reliably inferred from the $I(q)$. Whether the change in polydispersity is due to the LS process or some other interacting droplet effect, we have yet to determine with further experiments.

To conclude, we have identified a region of the phase diagram with qualitatively novel scattering intensity, $I(q)$. We have made the first observation, via light scattering and optical microscopy, of a monodisperse distribution of spherical droplets whose radius grows like $R \sim t^{1/2}$. We have developed a firm understanding of this growth law, and of the mechanism for the evolution of the monodisperse droplet distribution, in terms of a heterogeneous nucleation picture and a rate equation (2). We have identified the cloud point as the point at which there is a distinct change in morphology, from isolated spheres to continuously modulated phases, reminiscent of spinodal decomposition. At this point there is a large increase in the strength of the scattering and a spinodal ring appears in $I(q)$. Growth occurs via pattern coarsening, and the length scale behaves as $L \sim t^{1/3}$.

Monodisperse droplet formation allows unprecedented detail in the investigation of the kinetics of droplet growth. With some improvements to the apparatus we hope to quantify structural and depletion zone effects in $I(q)$. There are preliminary indications that these monodisperse spheres are generic. We have seen spherical form factors in shallow off-critical quenches in a simple nonpolymeric liquid system. We expect that this sort of nucleation and growth of monodisperse droplets will have technological significance.

We would like to thank D. Huse, J. Langer, and W. van Saarloos for their interest and insights into this problem, and J. Rosedal for invaluable assistance in sample preparation.

[1]J. S. Huang, W. I. Goldburg, and A. W. Bjerkaas, Phys. Rev. Lett. **32**, 921 (1974); Y. C. Chou and W. I. Goldburg, Phys. Rev. A **20**, 2105 (1979); **23**, 858 (1981); S. Krishnamurthy and W. I. Goldburg, Phys. Rev. A **22**, 2147 (1980).

[2]N. C. Wong and C. M. Knobler, J. Chem. Phys. **69**, 725 (1978); **85**, 1972 (1981); Phys. Rev. A **24**, 3205 (1981).

[3]P. Wiltzius, F. S. Bates, and W. R. Heffner, Phys. Rev. Lett. **60**, 1538 (1988); F. S. Bates and P. Wiltzius, J. Chem. Phys. **91**, 3258 (1989).

[4]T. Hashimoto, M. Itakura, and H. Hasegawa, J. Chem. Phys. **85**, 6118 (1986); T. Hashimoto, M. Itakura, and N. Shimidzu, J. Chem. Phys. **85**, 6773 (1986).

[5]P. Flory, *Principles of Polymer Chemistry* (Cornell Univ. Press, Ithaca, 1953).

[6]P.-G. de Gennes, *Scaling Concepts in Polymer Physics* (Cornell Univ. Press, Ithaca, 1979).

[7]J. W. Cahn and J. E. Hillard, J. Chem. Phys. **28**, 258 (1958); **31**, 688 (1959); J. W. Cahn, J. Chem. Phys. **42**, 93 (1965).

[8]See, for example, H. C. van de Hulst, *Light Scattering by Small Particles* (Dover, New York, 1981).

[9]I. M. Lifshitz and V. V. Slyozov, J. Phys. Chem. Solids **19**, 35 (1961).

[10]D. Huse, Phys. Rev. B **34**, 7845 (1986).

[11]This is discussed, e.g., by J. Hoffer and D. Sinha, Phys. Rev. A **33**, 1918 (1986).

[12]S. Hayware, D. W. Heermann, and K. Binder, J. Stat. Phys. **49**, 1053 (1987).

[13]E. Siggia, Phys. Rev. A **20**, 595 (1979).

[14]F. S. Bates, J. H. Rosedale, P. Stepanek, T. P. Lodge, P. Wiltzius, G. H. Fredrickson, and R. P. Hjelm (to be published).

[15]K. Binder, J. Chem. Phys. **79**, 6387 (1983).

[16]J. F. Joanny and L. Leiber, J. Phys. (Paris) **39**, 951 (1978).

[17]J. S. Langer and A. J. Schwartz, Phys. Rev. A **21**, 948 (1980).